OPEN

Citation: Cell Death and Disease (2014) 5, e1137; doi:10.1038/cddis.2014.66

www.nature.com/cddis

Longikaurin A, a natural ent-kaurane, induces G2/M phase arrest via downregulation of Skp2 and apoptosis induction through ROS/JNK/c-Jun pathway in hepatocellular carcinoma cells

Y-J Liao[1,5], H-Y Bai[1,2,5], Z-H Li[2,5], J Zou[3], J-W Chen[1], F Zheng[4], J-X Zhang[1], S-J Mai[1], M-S Zeng[1], H-D Sun[3], J-X Pu*[,3] and D Xie*[,1]

Hepatocellular carcinoma (HCC) is the most common form of primary liver cancer, and is also highly resistant to conventional chemotherapy treatments. In this study, we report that Longikaurin A (LK-A), an ent-kaurane diterpenoid isolated from the plant *Isodon ternifolius*, induced cell cycle arrest and apoptosis in human HCC cell lines. LK-A also suppressed tumor growth in SMMC-7721 xenograft models, without inducing any notable major organ-related toxicity. LK-A treatment led to reduced expression of the proto-oncogene S phase kinase-associated protein 2 (Skp2) in SMMC-7721 cells. Lower Skp2 levels correlated with increased expression of p21 and p-cdc2 (Try15), and a corresponding decrease in protein levels of Cyclin B1 and cdc2. Overexpression of Skp2 significantly inhibited LK-A-induced cell cycle arrest in SMMC-7721 cells, suggesting that LK-A may target Skp2 to arrest cells at the G2/M phase. LK-A also induced reactive oxygen species (ROS) production and apoptosis in SMMC-7721 cells. LK-A induced phosphorylation of c-Jun N-terminal kinase (JNK), but not extracellular signal-regulated kinase and P38 MAP kinase. Treatment with, the JNK inhibitor SP600125 prevented LK-A-induced apoptosis in SMMC-7721 cells. Moreover, the antioxidant N-acetylcysteine prevented phosphorylation of both JNK and c-Jun. Taken together, these data indicate that LK-A induces cell cycle arrest and apoptosis in cancer cells by dampening Skp2 expression, and thereby activating the ROS/JNK/c-Jun signaling pathways. LK-A is therefore a potential lead compound for development of antitumor drugs targeting HCC.

Cell Death and Disease (2014) **5,** e1137; doi:10.1038/cddis.2014.66; published online 20 March 2014
Subject Category: Cancer

Introduction

Hepatocellular carcinoma (HCC) is one of the most common malignancies reported worldwide, and accounts for 4.6% of all neoplasias. HCC is clinically resistant to conventional chemotherapy treatments, and is documented to have a 94% mortality rate.[1,2] There is thus an urgent need to develop more effective therapeutic agents to minimize both the incidence and severity of HCC.

Many anticancer agents dampen malignant growth by arresting the cell cycle at the G1, S or G2/M phases.[3] E3 ubiquitin ligases are a class of enzymes which regulate cell cycle progression, and changes in their activity can contribute to malignant cell proliferation.[4] S phase kinase-associated protein 2 (Skp2), is the F-box component of an E3 ubiquitin ligase, and may interact with several proteins, including $p21^{Cip1}$,[5–7] $p27^{Kip1}$,[8–10] $p57^{Kip2}$ and p130.[11,12] Skp2 function likely leads to degradation of tumor suppressor proteins, such as Cdk inhibitors p21 and p27, inducing formation of the Cdk complex and thereby accelerating cell cycle progression. Skp2 is detected at increased levels in several human cancers.[13]

There is compelling evidence that cellular adaptation to reactive oxygen species (ROS) stress has a part in maintaining a cellular cancer phenotype and chemotherapy resistance.[14] Even a modest increase in ROS levels can stimulate cell growth and proliferation.[15,16] However, excessive ROS production surmounts cellular antioxidant defenses, triggering apoptosis.[17] Interestingly, cancer cells are more sensitive to rapid increases in ROS levels than are normal cells. Oncogenic transformation elevates basal ROS levels

[1]Sun Yat-Sen University Cancer Center, State Key Laboratory of Oncology in South China, Collaborative Innovation Center for Cancer Medicine, Guangzhou, China; [2]Department of Forensic Medicine, Zhongshan School of Medicine, Sun Yat-Sen University, Guangzhou, China; [3]State Key Laboratory of Phytochemistry and Plant Resources in West China, Kunming Institute of Botany, Chinese Academy of Sciences, Kunming, China and [4]Medical Research Center, Sun Yat-Sen Memorial Hospital, Guangzhou, China
*Corresponding authors: D Xie, State Key Laboratory of Oncology in South China, Sun Yat-Sen University Cancer Center, No. 651, Dongfeng Road East, Guangzhou 510060, China. Tel: +86 20 87343193; Fax: +86 20 87343170; E-mail: xied@mail.sysu.edu.cn
or J-X Pu, State Key Laboratory of Phytochemistry and Plant Resources in West China, Kunming Institute of Botany, Chinese Academy of Sciences, No. 132, Lanhei Road, Heilongtan, Kunming 650204, China. Tel: +86 871 65223616; Fax: +86 871 65223223; E-mail: pujianxin@mail.kib.ac.cn
[5]These authors contributed equally to this work.
Keywords: Longikaurin A; hepatocellular carcinoma; cell cycle arrest; apoptosis; Skp2
Abbreviations: LK-A, Longikaurin A; HCC, hepatocellular carcinoma; ROS, reactive oxygen species; JNK, c-Jun N-terminal kinase; ERK, extracellular signal-regulated kinase; NAC, N-acetylcysteine
Received 21.10.13; revised 15.1.14; accepted 27.1.14; Edited by M Agostini

significantly so that any further acute increases can trigger reactivation of the apoptotic program in cancer cells.[18] Production of abnormal amounts of ROS interferes with cellular signaling pathways by free radical targeting of cellular macromolecules including proteins and DNA, as well as by triggering cell cycle arrest and apoptosis.[19,20]

Diterpenoid compounds are established to have a crucial role in cancer chemotherapy. *Isodon ternifolius* (D. Don) Kudô, a prominent species of the Isodon genus, is known for producing bioactive ent-kaurane diterpenoids,[21–23] and has long been used as folk medicine for the treatment of icterohepatitis, enteritis and other inflammatory conditions.[24] *I. ternifolius* is also the major ingredient of a Chinese patent medicine 'FufangSanyexiangchacaiPian', which is used to treat acute and chronic hepatitis and hepatitis B. Longikaurin A (LK-A), shown in Figure 1a, is a major *ent-kaurane* diterpenoid produced by *I. ternifolius*.[25] To the best of our knowledge, the effectiveness of LK-A treatment on HCC has not been reported.

In the present study, we observed that LK-A inhibited both *in vivo* and *in vitro* proliferation of HCC. We further explored the mechanism by which LK-A may inhibit malignant proliferation, such as by downregulating Skp2 and inducing cell cycle arrest, and by causing apoptosis activated by ROS/c-Jun N-terminal kinase (JNK)/c-Jun signaling pathway induction. Collectively, our data suggests that the diterpenoid LK-A has significant potential as an antitumor agent for HCC.

Results

LK-A suppresses cell growth in HCC, and triggers cell cycle arrest at the G2/M phase. We used the HCC cell lines BEL-7402, SMMC-7721, Huh7 and HepG2 to investigate the effects of LK-A on HCC. As shown in Figure 1b, LK-A substantially inhibited HCC cell growth in a time and dose-dependent manner. In contrast, LK-A displayed only moderate cytotoxicity toward the normal liver cell line LO2. We decided to use SMMC-7721 and HepG2 cells for further investigation as part of this study. In addition, colony formation assays demonstrated that SMMC-7721 and HepG2 cells treated with LK-A for 36 h formed both fewer and smaller colonies than did control liver cells (Figure 1c), indicating that LK-A inhibits growth of the two HCC cell lines. To further examine the mechanism by which LK-A may inhibit proliferation of SMMC-7721 and HepG2 cells, we studied the effects of LK-A on cell cycle arrest. SMMC-7721 and HepG2 cells were incubated with varying concentrations of LK-A for 36 h, stained with propidium iodide, and analyzed by flow cytometry. Indeed, LK-A treatment led to a dose-dependent induction of cell cycle arrest in the G2/M phase arrest (Figure 1d).

LK-A induces apoptosis of HCC cells. To further probe LK-A inhibition of cell proliferation and colony formation, we used Hoechst 33342 staining to assess LK-A-dependent changes in cell morphology. SMMC-7721 and HepG2 cells treated with LK-A for 36 h displayed dramatically changed morphologies (Figure 2a). Arrowheads indicate cells exhibiting chromatin condensation, indicating the induction of apoptosis (Figure 2a). To determine if LK-A has a pro-apoptotic effect on HCC cells, flow cytometry analysis via Annexin V/PI staining was performed. Flow cytometry analysis indicated that LK-A-treated HCC cells undergo apoptosis at significantly higher rates than control cells (Figure 2b). Furthermore, western blot analysis suggested a significant LK-A dose-dependent decrease in levels of pro-caspase-3, caspase-8, and an increase in cleaved Caspase-3, cleaved PARP (Figure 2c). Together, these results demonstrate that LK-A can induce apoptosis of HCC tumor cells.

Skp2 may have a major role in LK-A-induced SMMC-7721 G2/M phase arrest. To obtain further insight into the mechanisms of LK-A in SMMC-7721 cell cycle arrest, messenger RNA (mRNA) expression profiles of LK-A treated cells for 36h were compared with those of none treated cells using a human cell cycle RT^2 profiler PCR array containing 84 cell cycle-related genes. The results showed a total of three upregulated (*CDKN1A*, *CDKN1B* and *GADD45A*) and five downregulated (*CCNB1*, *CDC2*, *CDK2*, *MKI67* and *Skp2*) genes, classified as such by a more than two-fold change in mRNA levels (Figure 3a, Supplementary Table 1). These targets were subsequently validated by a western blotting assay. Consistent with mRNA expression levels determined by real-time PCR, SMMC 7721 cells treated with LK-A displayed a decrease in Skp2 protein levels (Figure 3b). Skp2 is an E3 ubiquitin ligase, which may interact with several members of the Cdk complex and induce cell cycle progression by degradation of CDK inhibitors, such as p21 and p27. It has been previously shown that Skp2 downregulation leads to cell cycle arrest.[26–28] Here we further show by western analysis that Skp2 downregulation is accompanied by an increase in p21, p-cdc2 and Mty1 levels, and that p-Wee1 and CyclinB1 are decreased, but levels of p27 are nearly unchanged (Figure 3b).

To further explore the role of Skp2 in induction of cell cycle arrest, we constructed a pcDNA-SKP2 overexpression vector. Western blot analysis indicated that Skp2 overexpression leads to decreases in protein levels p21 and p-cdc2, but that the expression of CyclinB1 and cdc2 was elevated (Figure 3c). As shown in Figure 3d, Skp2 overexpression nearly reverses the cell cycle arrest induced by LK-A. These results confirmed that Skp2 may have a major role in LK-A-induced G2/M phase arrest.

The role of ROS generation in LK-A-induced cell apoptosis. Cellular ROS generation can significantly impact the effects of various anticancer agents on tumor cell apoptosis.[18,29] We therefore used the fluorescent probe 20,70-dichlorofluorescindiacetate (DCFH/DA) to monitor intracellular ROS levels in the presence and absence of LK-A. We found that LK-A-treated cells had significantly higher levels of ROS than did control cells (Figure 4a). We next set out to determine if increased ROS production impacts LK-A-induced apoptosis. Cells were treated with the antioxidant N-acetylcysteine (NAC) at 1 h before adding LK-A and incubation for an additional 36 h. We found that pretreatment with NAC caused a significant decrease in the levels of LK-A-induced cell apoptosis (Figure 4b). Moreover, blocking ROS production by NAC resulted in an increase in pro-caspase-3, caspase-8 and a decrease in

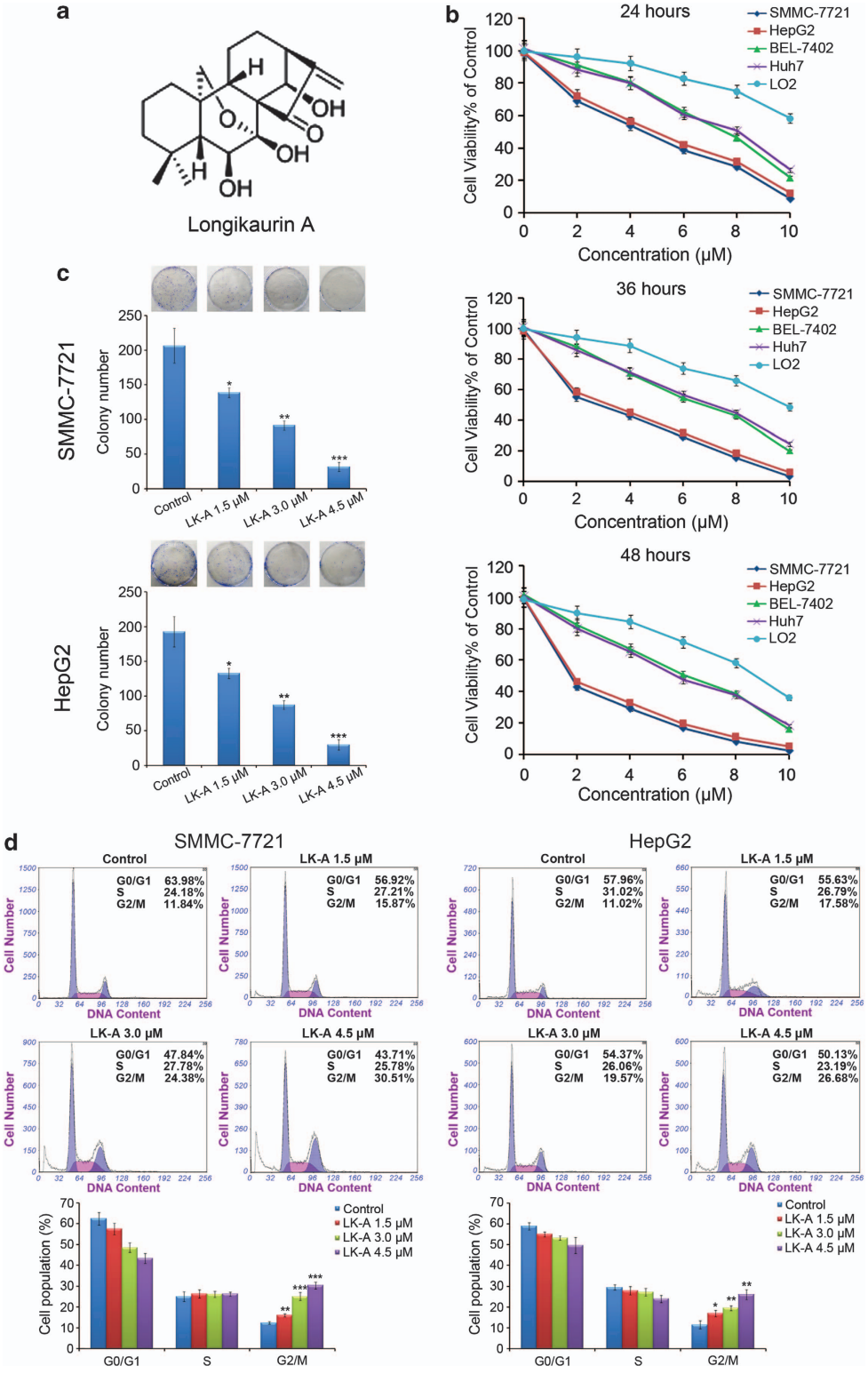

Figure 1 LK-A inhibits cells proliferation and induces G2/M arrest in SMMC-7721 and HepG2 cells. (**a**) Chemical structure of LK-A. (**b**) HCC cells proliferation was assessed by PrestoBlue. Cells were treated with 0, 2, 4, 6, 8 and 10 μM of LK-A for 24, 36 and 48 h. At 36 h, IC_{50} value for each cell lines determined from PrestoBlue results are as follows: SMMC-7721 = 2.75 μM, HepG2 = 5.13 μM, BEL-7402 = 6.83 μM, Huh7 = 7.12 μM and LO2 = 9.69 μM. (**c**) SMMC-7721 and HepG2 cells colonied formation with or without LK-A treatment. (**d**) LK-A caused a G2/M arrest. Cells were treated with DMSO and varying concentrations of LK-A (0, 1.5, 3.0, 4.5 μM) for 36 h. The cell cycle distributions were analyzed by flow cytometry. Histograms display the percentage of cell cycle distribution. Cell Number, peak value of phase; Columns, means; bars, S.D. ($n = 3$). *$P < 0.05$, **$P < 0.01$ and ***$P < 0.001$, significantly different compared with control by *t*-test

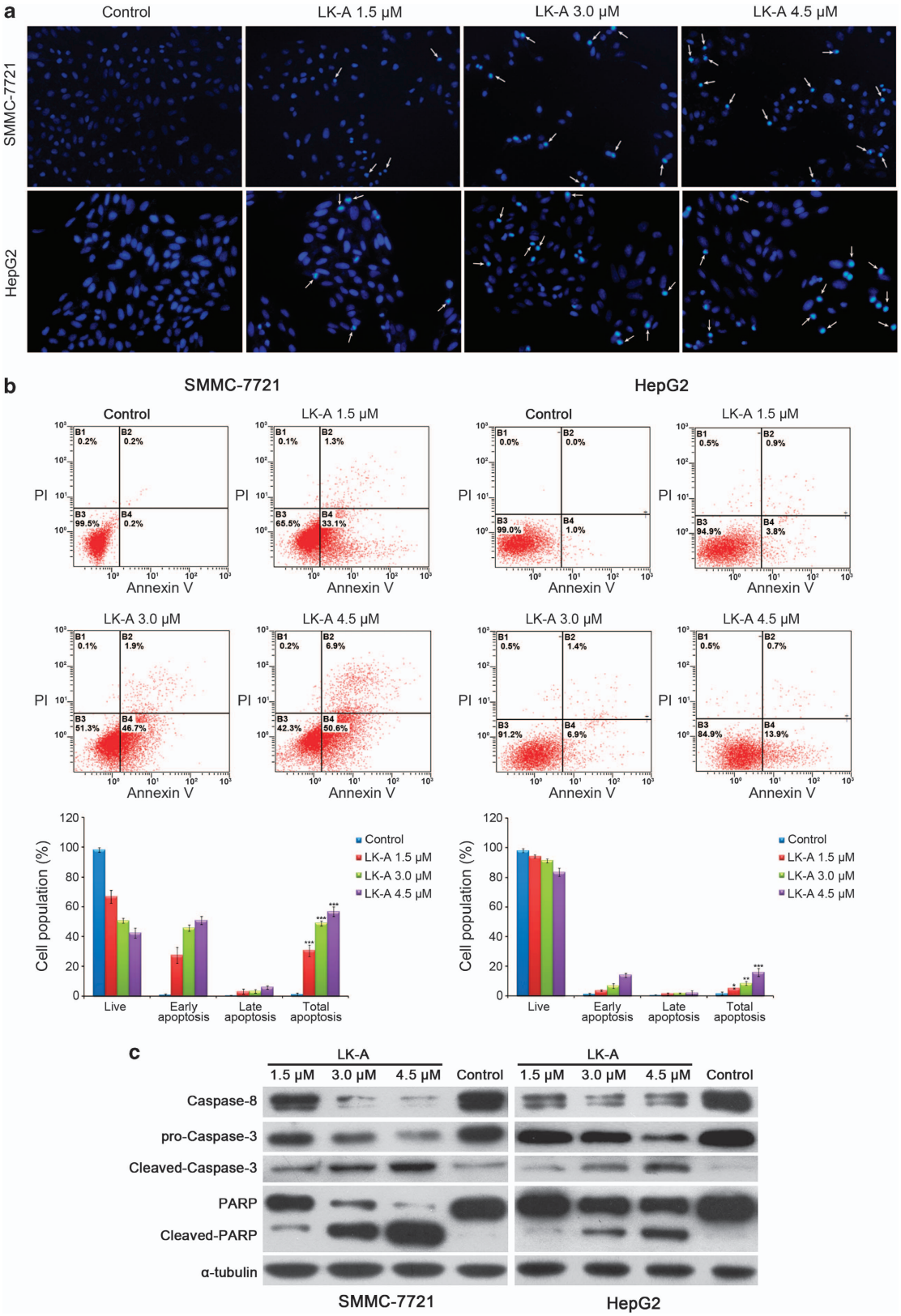

Figure 2 Evidence that LK-A induced apoptosis. (**a**) Cell morphological alterations and nuclear changes associated with SMMC-7721 and HepG2 cells after LK-A treatment were assessed by staining with Hoechst 33342 and visualized by fluorescence microscopy. (**b**) FACS analysis via Annexin V/PI staining was used to identify apoptosis induced by LK-A. The percentage of cell cycle distribution was shown as the mean ± S.D. from three independent experiments. $^{*}P<0.05$, $^{**}P<0.01$ and $^{***}P<0.001$. (**c**) Cells were treated with or without various concentrations of LK-A for 36 h. Caspase-3, -8, and PARP levels were determined by western blot

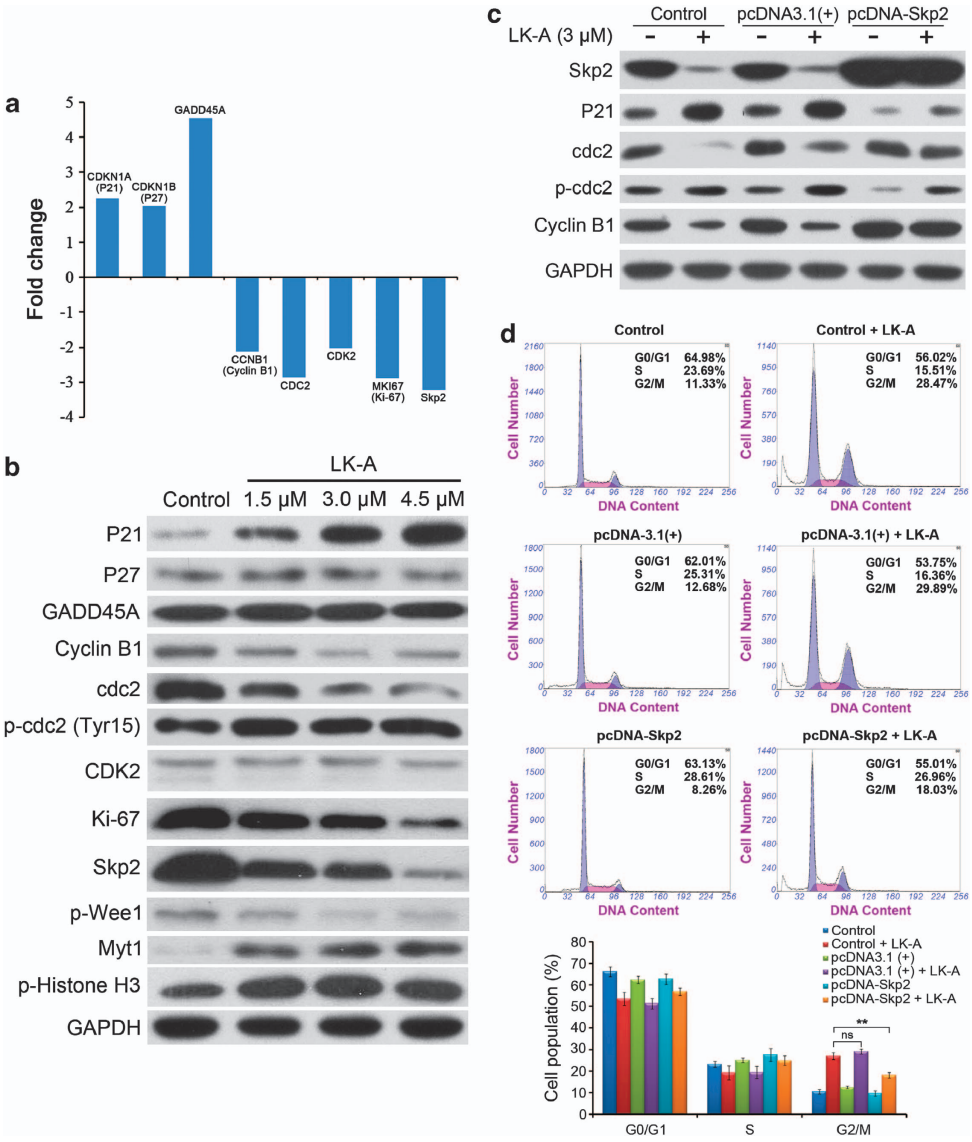

Figure 3 LK-A induces SMMC-7721 G2/M phase arrest though downing regulation of Skp2. (**a**) The fold change in cell cycle-related genes after LK-A treated for 36 h. (**b**) SMMC-7721 cells were treated with or without LK-A for 36 h. The expression of cell cycle-related proteins were measured by western blot. (**c**) SMMC-7721 cells were transfected with pcDNA-SKP2 and pcDNA3.1 (+), respectively. After treatment with 3 μM LK-A for 36 h, protein lysates were prepared and analyzed by western blot. (**d**) After transfection and treatment with 3 μM LK-A 36 h, the cell cycle distribution of SMMC-7721 cells were determined by flow cytometry. Cell Number, peak value of phase. The percentage of cell cycle distribution was shown as the mean ± S.D. from three independent experiments. $^{**}P<0.01$; ns, not significant

cleaved Caspase-3, cleaved PARP expression (Figure 4c). Together, these results suggest that ROS accumulation is necessary and mediates LK-A-induced apoptosis in SMMC-7721 cells.

LK-A-dependent ROS accumulation activates the JNK/c-Jun pathway. MAPK signaling cascades regulate not only cell growth, differentiation and development, but also apoptosis.[30,31] To examine the mechanism by which LK-A affects MAP kinase activation, the role of LK-A in the activation of extracellular signal-regulated kinase (ERK), JNK and p38 MAP kinase was investigated. As shown in Figure 4d, phosphorylation levels of both JNK and c-Jun gradually, and significantly, increased after LK-A treatment. However, there was no discernible change in phosphorylation levels of ERK and p38. As Figures 4e and f demonstrate, the JNK inhibitor SP600125 significantly restored cellular apoptosis in response to LK-A. As ROS production could determine the fate of cancer cells through regulating a number of cellular pathways,[32] we examined if ROS accumulation is involved in the activation of JNK/c-Jun pathway in our model system. Western blot analysis showed that pretreatment with NAC nearly reversed the phosphorylation of JNK and c-Jun (Figure 4g). These results illustrate that the apoptosis of SMMC-7721 cells induced by LK-A is mediated by the activation of the ROS/JNK/c-Jun pathway.

LK-A suppressed the tumor growth in mouse xenograft models. To further evaluate the role of LK-A in tumor proliferation *in vivo*, 3×10^6 SMMC-7721 cells were

subcutaneously inoculated into nude mice. Mice were treated every 3 days with LK-A at 3 and 6 mg/kg intraperitoneally, 5-FU (positive control), or dimethylsulfoxide (DMSO) (negative control) for 4 weeks. LK-A significantly inhibited the growth of tumor xenografts (Figure 5a) with the tumor weight of LK-A (3 and 6 mg/kg)-treated mice significantly less than that of the

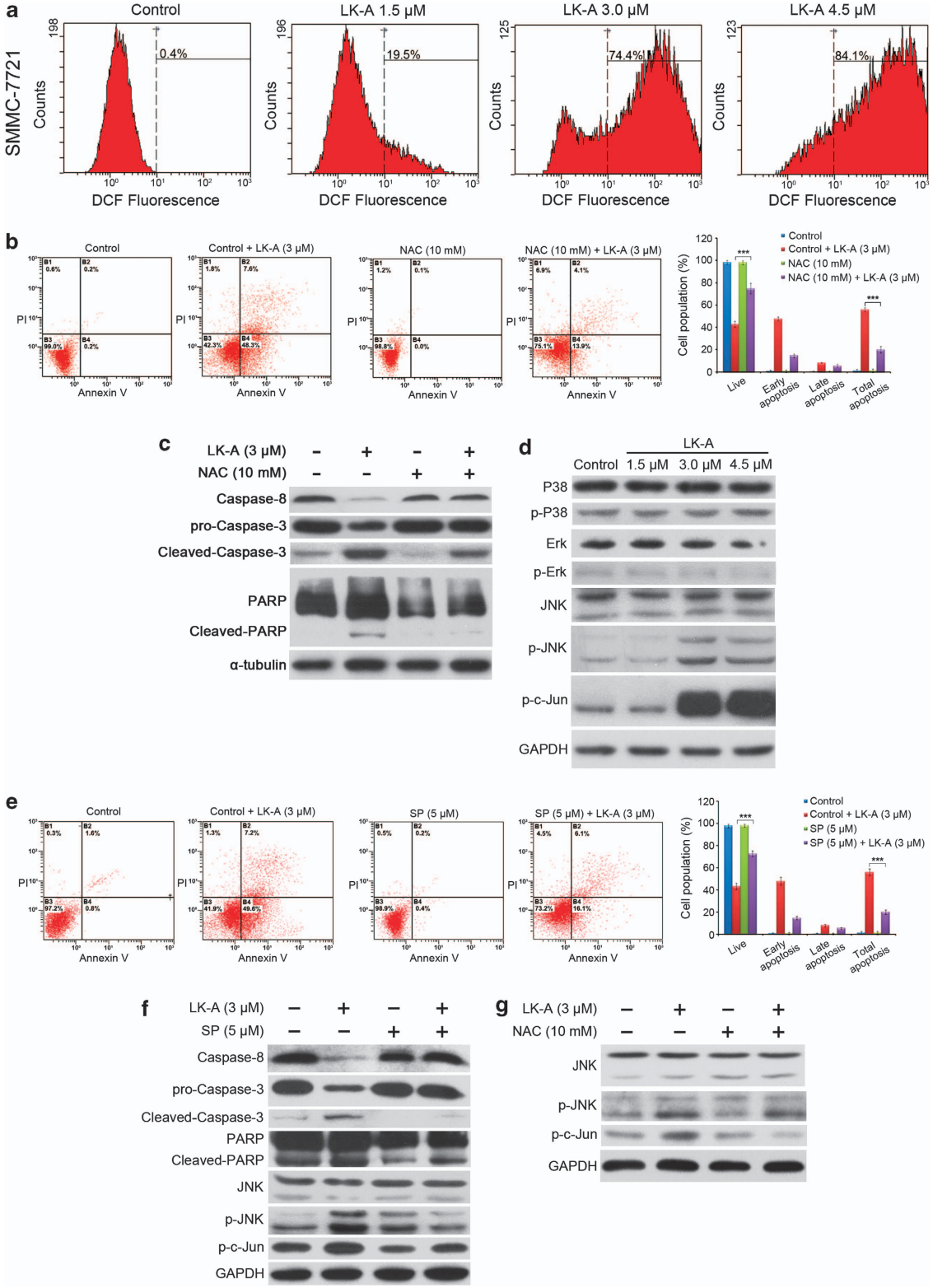

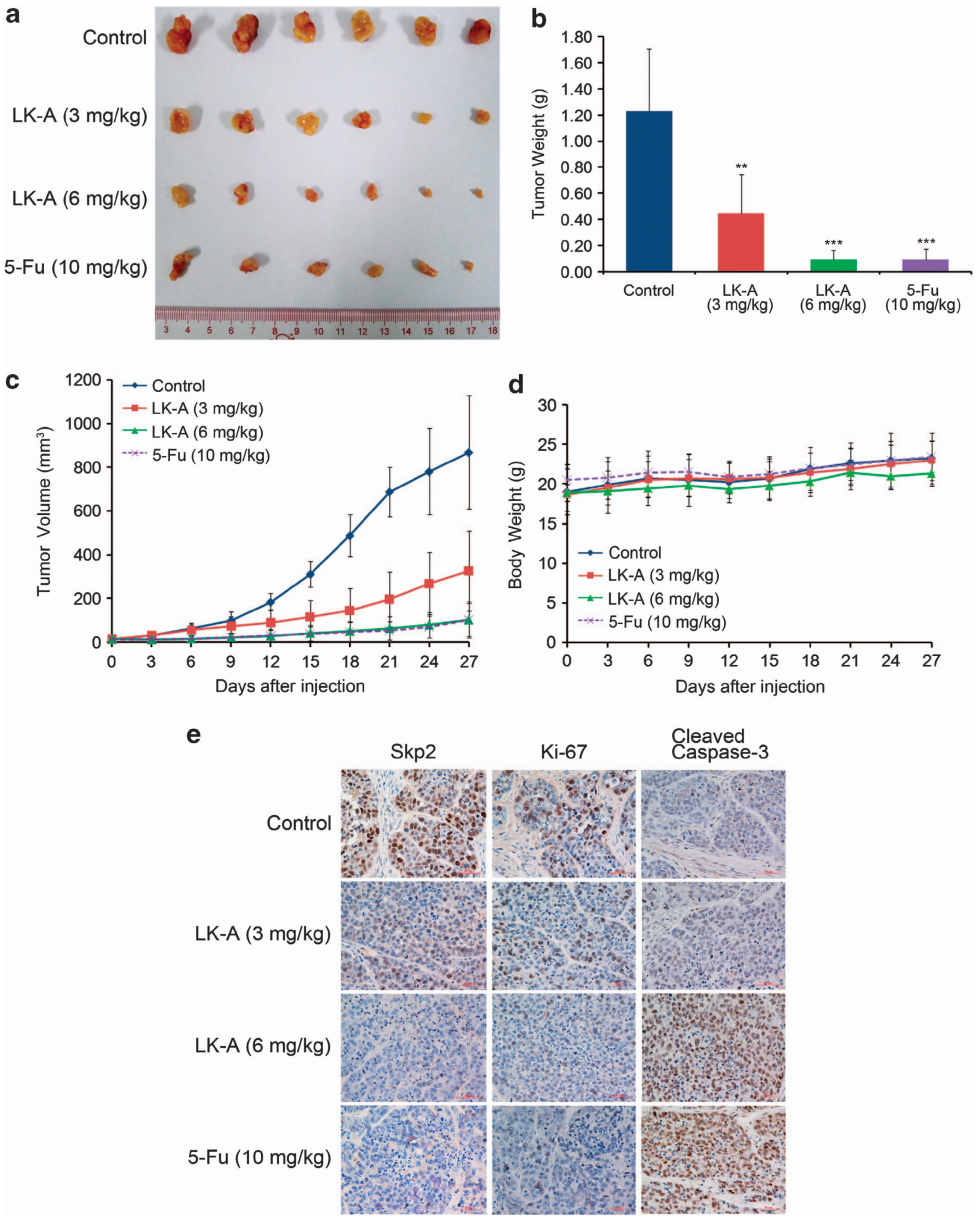

Figure 5 LK-A inhibits liver cancer tumor xenograft growth *in vivo*. (**a**) SMMC-7721 cells were subcutaneously inoculated into the right flank of nude mice. The mice were randomly divided into four groups ($n = 6$) and treated intraperitoneally with LK-A (3 mg/kg or 6 mg/kg), 5-Fu (10 mg/kg) and DMSO (dissolved in sodium chloride, control) every 3 days for 4 weeks. The resulting tumors were excised from the animals after treatment. (**b**) LK-A treatment resulted in significantly lower tumor weight compared with controls. $^{**}P < 0.01$, $^{***}P < 0.001$. (**c** and **d**) Tumor volumes and body weights were measured every 3 days for 4 weeks. (**e**) The cleaved Caspase-3, Skp2 and Ki-67 expression in tumor xenograft tissues was examined using immunohistochemistry

Figure 4 The accumulation of ROS production induced by LK-A is required for cell apoptosis and necessary for activating JNK/c-Jun pathway. (**a**) Effect of LK-A on ROS generation. SMMC-7721 cells were loaded with DCFH/DA for 30 min and then treatment with LK-A for 3 h. The mean DCF fluorescence was measured by flow cytometry. (**b**) Cells were pre-incubated for 1 h in the presence or absence of NAC (10 mM), and then LK-A (3 μM) and incubated for 36 h. Induction of apoptosis was determined by flow cytometry. The data shown represent means ± S.D. of three independent experiments. $^{***}P < 0.001$ versus NAC-treated control group. (**c**) Effects of NAC on the expression of Caspase-3, -8 and PARP. Protein lysates were prepared from SMMC-7721 cells after treatment with 3 μM LK-A for 36 h in the presence or absence of NAC and analyzed by western blot. (**d**) Effects of LK-A on ERK, JNK and p38 MAP kinase activation in SMMC-7721 cells. SMMC-7721 cells were treated with various concentrations (0, 1.5, 3.0, 4.5 μM) of LK-A for 36 h and analyzed by western blot. (**e**) Cells were pre-incubated for 1 h in the presence or absence of SP600125 (5 μM), and 3 μM LK-A was added for an additional 36 h. The percentage of cell apoptosis was shown as the mean ± S.D. from three independent experiments. $^{***}P < 0.001$ compared with SP-treated control group, SP, SP600125. (**f**) Cells were pre-incubated for 1 h in the presence or absence of SP600125 (5 μM), and then treated with 3 μM LK-A for 36 h, followed by western blot analysis of apoptosis-related proteins. (**g**) Cells were pre-incubated for 1 h in the presence or absence of NAC (10 mM), and then treated with 3 μM LK-A for 36 h, followed by western blot analysis of JNK/p-JNK and c-Jun expression

negative control group (Figure 5b). The mean tumor volume for negative control mice increased from 12.81 ± 3.11 to $868.21 \pm 258.48\,mm^3$, whereas LK-A-treated mice at 3 and 6 mg/kg treatment increased from 13.78 ± 2.59 to $326.1 \pm 182.65\,mm^3$ and 13.12 ± 3.26 to $101.17 \pm 82.28\,mm^3$, respectively, while the 5-FU mice increased from 12.72 ± 2.93 to $102.04 \pm 75.72\,mm^3$ (Figure 5c). By contrast, there was no significant loss in body weight in the experimental animals (Figure 5d). The immunohistochemistry staining of excised tumor sections revealed a higher expression of cleaved Caspase-3, but the lower expression of Skp2 and Ki-67 in LK-A-treated tumors (Figure 5e) consistent with the *in vitro* results. To investigate any potential cytotoxic effects of LK-A on normal tissues, non-tumor-bearing mice were intraperitoneally treated with LK-A (6 mg/kg) and DMSO (negative control) every 3 days for 4 weeks and there was no significant loss in body weight (data not shown). Furthermore, H&E staining of the organs collected at the end of the study also suggested no major organ-related toxicities (Figure 6).

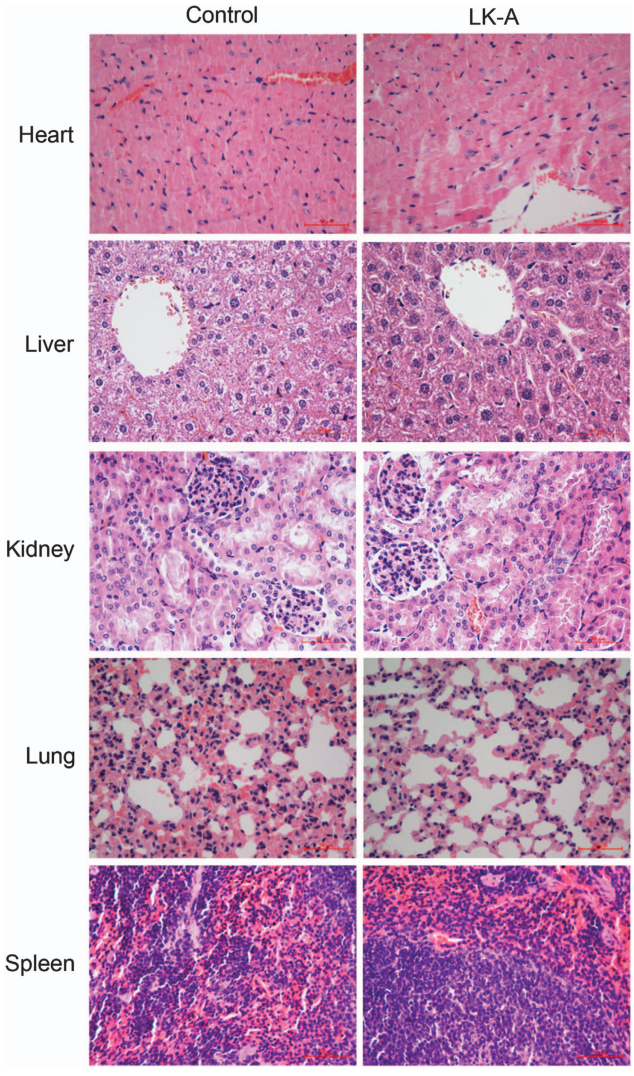

Figure 6 No obviously organ-related toxicity was found. Non-tumor-bearing mice were intraperitoneally treated with LK-A (6 mg/kg) or DMSO (dissolved in sodium chloride, control) every 3 days for 4 weeks. After the experiment, animals were sacrificed and the organs were fixed in formalin overnight and processed for paraffin embedding. The paraffin-embedded blocks were sectioned and stained by hematoxylin and eosin

Discussion

As current HCC therapies have limited effectiveness and exhibit intolerable toxicities in most cases, natural products and their derivatives are pursued as new and ideal sources for anti-HCC drugs discovery.[33–35] The unique carbon skeleton and multiple pharmacological properties of diterpenes have recently gained attention as new candidates against human cancers.[36,37] *I. ternifolius* is the major ingredient of a Chinese patent medicine 'FufangSanyexiangchacaiPian', which is currently used to treat acute and chronic hepatitis and hepatitis B. LK-A (Figure 1a), an ent-kaurane diterpenoid obtained from *I. ternifolius*, has a similar structure to diterpenes, which anti-nasopharyngeal carcinoma has been reported recently.[38] However, in this study, we examined LK-A treatment in HCC models and revealed a significant suppression of tumor growth both *in vivo* and *in vitro*. Moreover, this compound triggered cell cycle arrest at G2/M phase and induced cell apoptosis. We also discovered that LK-A results in G2/M arrest via downregulation of Skp2 and inducing apoptosis through ROS/JNK/c-Jun apoptotic pathway in SMMC-7721 cells.

The decreased formation of cdc2/Cyclin B1 complex inhibits cell-cycle progression from the G2 phase to the M phase.[39] LK-A treatment in SMMC-7721 cells resulted in G2/M phase arrest in a dose-dependent manner, reduced cdc2, cyclinB1 protein levels and increased the expression of p-cdc2 and p-histone3. During G2 phase, the cdc2/Cyclin B1 complex is kept inactive via phosphorylation at Thr14 and Tyr15 of cdc2 by Myt1 and Wee1, respectively.[40–42] The Cip and Kip family of CDK inhibitors p21 also participates in the G2 checkpoint. P21 could inhibit CDK1 activity through binding to the CDK1/CyclinB1 complex and inducing G2 phase arrest.[43–45] In the present study, the expression of p-Wee1 decreased, but the protein levels of Mty1 and p21 were increased. Next, we focused on understanding how LK-A reduced the activation of cdc2/CyclinB1 complex. Skp2, an F-box component of E3 ubiquitin ligases, has an essential role in the regulation of cell cycle progress.[27,46,47] Moreover, many studies demonstrate that Skp2 can serve as a therapeutic target in various cancers by mediating the cytostatic and cytotoxic effects of different chemotherapeutic drugs.[48] In this study, we discovered that LK-A downregulation of Skp2 subsequently increased the expression of p21. Consistent with this data, the overexpression of Skp2 nearly blocked any LK-A-induced upregulation of p21 and p-cdc2 protein levels and decreased cdc-2 and CyciInB1 protein levels. Our data suggest that downregulation of Skp2 by LK-A is essential for LK-A-induced cell cycle arrest.

Apoptosis, a fundamental process essential for development and maintenance of tissue homeostasis, is also a major route to eradicate cancer cells.[49] Nowadays, an effective strategies for cancer prevention and treatment is targeting of

the signaling intermediates in apoptosis.[50] In this work, we revealed that LK-A treatment induced a dose-dependent apoptosis in HCC cells. We also saw that LK-A treatment resulted in a significant decrease of pro-caspase-3, caspase-8 and increase of proteolytic cleavage of Caspase-3 and PARP.

Recently, studies have showed that excessive ROS production, induced by exogenous agents, will cause cellular apoptosis through the activation of signaling pathway, which results in selectively killing cancer cells.[51–53] LK-A induced a significant increase in ROS production in SMMC-7721 cells, while pretreatment with the ROS inhibitor NAC partially abrogates the LK-A-induced increase of apoptosis. Interestingly, NAC similarly abolished the LK-A effects on pro-Caspase3, cleaved Caspase-3, Caspase-8 and cleaved PARP. These results demonstrate that the induction of ROS is a critical upstream event for LK-A-induced SMMC-7721 apoptosis. Furthermore, we examined the levels of DNA damage-related proteins, such as phosphorylated ataxia telangiectasia mutated (p-ATM), phosphorylated ataxia telangiectasia and Rad3-related (p-ATR), CDC25A, CDC25C and Cyclin F, before and after LK-A treatment in SMMC-7721 cells. We found that after the treatment of LK-A, the levels of p-ATR and p-ATM were all substantially increased, and meanwhile, the levels of CDC25C decreased (Supplementary Figure S1). These data, taken together, suggest that LK-A treatment might activate DNA damage in HCC cells, and ultimately leads cancer cells to apoptosis. Clearly, further work is needed to clarify the mechanisms of LK-A to regulate DNA damage-induced HCC cell apoptosis in detail.

Various apoptotic stimuli can rapidly activate MAPKs, which include JNK, ERK and p38MAPK.[54–57] In SMMC-7721 cells, treatment with LK-A did not change p38 and ERK phosphorylation but the levels of phospho-JNK increased in a dose-dependent manner. Surprisingly, JNK activation is involved in the events of LK-A-mediated apoptosis, which was confirmed by the use of the JNK inhibitor SP600125. Until now, considerable evidences suggested that JNK is primarily activated by various environmental stresses including: UV radiation, osmotic shock, heat shock, oxidative stress, chemotherapeutic agents and protein synthesis inhibitors, among these, oxidative stress is particularly important.[58] So we investigated the activation of JNK with ROS elevation during LK-A treatment. Interestingly, our results showed that pretreatment with NAC in SMMC-7721 cells abolished the JNK/c-Jun activation by LK-A treatment. From these data, we concluded that LK-A induced apoptosis through ROS-dependent JNK/c-Jun apoptotic pathway.

In conclusion, this study presented an ent-kaurane diterpenoid LK-A from *I. ternifolius*, which inhibited the proliferation of HCC cells and SMMC-7721 xenograft tumor growth. *In vitro*, LK-A significantly induce cell cycle arrest at G2/M phase and apoptosis. Moreover, in SMMC-7721 cells, the agent arrests cell cycle at the G2/M phase through downregulation of Skp2, and induces apoptosis via the ROS-dependent JNK /c-Jun pathway. In the SMMC-7721 cells xenograft model, LK-A showed significant antitumor activity with low levels of toxicity. This compelling evidence suggests that LK-A is great candidate for the development of new chemotherapy agents for the treatment of human HCC.

Materials and Methods

Materials. *I. ternifolius* (D. Don) Kudô leaves were collected in Jinxiu, Guangxi, China. Ten kilogram of dried and milled plant material was subject to extraction at room temperature four times with 100 l 70% aqueous Me_2CO, for 3 days each time, and then filtered. The filtrate was then evaporated under reduced pressure and partitioned four times with 60 l of EtOAc. The substrate from the EtOAc partition (938.5 *g*) was applied to silica gel (200–300 mesh) and eluted with $CHCl_3$–Me_2CO (1 : 0–0 : 1), to give six fractions, A–F. Fraction B (618.5 *g*) was decolorized on an MCI gel and eluted with 90% MeOH–H_2O to yield fractions B1–B4. Fractions B1 (116 *g*) and B2 (135 *g*) were further separated by repeated silica gel column chromatography to produce LK-A (20 *g*). The final LK-A concentrate was dissolved in DMSO to a concentration of 50 mM and stored at $-20\,^{\circ}C$. Working concentrations of 1.5, 3.0 and 4.5 μM LK-A were prepared freshly before each experiment by dilution in media. All cell culture reagents were purchased from Gibco (Grand Island, NY, USA). PrestoBlue, DCFH/DA, the BCA protein assay kit, Lipofectamine 2000, the Annexin V-FITC apoptosis detection kit and the cell cycle detection kit were all purchased from Life Technologies (Grand Island, NY, USA). NAC was purchased from MP Biomedicals (Santa Ana, CA, USA). The JNK inhibitor (SP600125) was purchased from Sigma (St. Louis, MO, USA). Cyclin F antibody was purchased from Signalway Antibody LLC (College Park, MD, USA), and the other antibodies used in this study were purchased from Cell Signaling Technologies Inc. (Danvers, MA, USA).

Cell culture. The HCC cell lines, HepG2 and Huh7, and the normal hepatic cell line LO2, were cultured in Dulbecco's modified Eagle's medium, supplemented with 10% fetal bovine serum (FBS) and incubated at 37 °C with 5% CO_2, and 95% humidity. HCC cell lines SMMC-7721, and BEL-7402 were maintained in RPMI 1640 supplemented with 10% FBS.

Cell viability assay. The effect of LK-A on cell viability was assessed by using the PrestoBlue indicator. A total of 3×10^3 cells/well were seeded in 96-well plates overnight and then treated with varying concentrations of LK-A (0, 2, 4, 6, 8, 10 μM). In order to minimize any effects of the solvent on cell viability, the final concentration of DMSO was kept to $<0.05\%$ in all wells. Cells were either incubated for 24, 36 or 48 h at 37 °C in a humidified incubator, and then 10 μl PrestoBlue reagent was added into each well and incubated for another 40 min. Absorbances were measured at 570 and 600 nm in each well by a microplate spectrophotometer (SpectraMax M5, Molecular Devices, Sunnyvale, CA, USA).

Colony formation assay. SMMC-7721 and HepG2 cells were plated as 10^3 cells/well in six-well plates and maintained with or without LK-A for 1 week. After growth, colonies were fixed with methanol for 30 min and stained with 0.1% crystal violet for visualization and counting.

Detection of the cell cycle stage. To determine the distribution of cell cycle stages, control and treated cells were collected into polypropylene tubes and pelleted at 2000 rpm for 5 min. Cells were then washed with phosphate-buffered saline (PBS) and fixed with chilled 70% ethanol for 48 h at 4 °C. Fixed cells were washed with PBS and incubated with RNase A (50 μg/ml) for 30 min followed by incubation with propidium iodide (50 μg/ml) for 30 min at room temperature. Cell cycle analysis was performed on a Coulter Epics XL flow cytometry system (Beckman Coulter, Miami, FL, USA). In total, 15 000 events were recorded in each analysis. The percentage of cells either at G0/G1, S or G2/M stages was calculated using MultiCycle AV for Windows Version 295 (Beckman Coulter).

Hoechst 33342 staining for morphological evaluation. Approximately 5×10^4cells/well were plated in six-well plates, and the cells were then incubated with (0, 1.5, 3.0 or 4.5 μM) LK-A for 36 h. After incubation, cells were washed with PBS, fixed in 4% paraformaldehyde for 30 min and then stained with 20 μg/ml Hoechst 33342 for 15 min at room temperature in the dark. Cells were then assessed by fluorescence microscopy for morphological changes after LK-A treatment.

Apoptosis detection by flow cytometry. The percentage of apoptotic cells was determined by using an Annexin V-FITC apoptosis detection kit, as per the manufacturer's protocol. After LK-A or mock treatment, cells were harvested, washed in cold PBS and then pelleted. Cells were stained in the dark for 15 min at room temperature, and analyzed by flow cytometry within 1 h of ending the staining procedure. Data were analyzed by CXP Analysis Software Version 2.0 (Beckman Coulter).

Real-time PCR gene array. RNA was extracted from LK-A treatment and none treatment SMMC-7721 cells using Trizol (Invitrogen, Carlsbad, CA, USA) and we cleaned them using the RNeasy MinElute cleanup kit (Qiagen, Valencia, CA, USA). Subsequently, total RNA was reverse transcribed using SuperScript III reverse transcriptase (Invitrogen) and cDNA was amplified by PCR using 2 × Super Array PCR master mix (SABiosciences, Frederick, MD, USA). Real-time PCR was then performed on each sample using the Human Cell Cycle RT^2 Profiler PCR array (PAHS-020A; SABiosciences) on an ABI 7900HT real-time PCR system (Applied Biosystems, Grand Island, NY, USA) according to the manufacturer's instructions. Data were normalized for GAPDH levels by the ΔΔCt method.

Measurement of ROS production. Intracellular ROS production was detected by using the peroxide-sensitive fluorescent probe DCFH-DA. In brief, cells were first incubated with DCFH-DA (10 μmol/l) at 37 °C for 30 min and then treated with LK-A for 3 h. Cells were then washed twice and resuspended in PBS to measure ROS accumulation by flow cytometry.

Construction of the Skp2 overexpression vector. To generate the pcDNA-Skp2 overexpression vector, a fragment of Skp2 was PCR amplified from the cDNA of SMMC-7721 cells, using the following primers: forward 5′-CTAGCTA GCGCCACCATGCACAGGAAGCACCTCCAG-3′, reverse 5′-CCGGAATTCTCAG ACGTTACTTTCACCGTGCC-3′.

Transfection of SMMC-7721 cells with pcDNA-Skp2. Cells were transfected using Lipofectamine 2000, as per the manufacturer's protocol. Twenty-four hours post transfection, cells were treated with LK-A and cultured for an additional 36 h, prior to collection for western blot and flow cytometric analyses.

Western blotting assay. Cells were harvested from plates by gentle scraping lysed, and stored at − 80 °C. Protein concentrations were measured by the BCA Protein Assay. Fifty milligram of protein from each sample was subject to SDS-PAGE, transferred electrophoretically to 0.45 μm polyvinylidene fluoride (PVDF) membrane and subsequently incubated in blocking buffer (5% nonfat dry milk) for 1 h at room temperature. PVDF membranes were incubated with appropriate primary antibody overnight at 4 °C, washed and incubated with secondary antibody for 2 h at room temperature. Specific antibody binding was detected by chemiluminescence detection.

Vivo **tumor xenograft study.** Six-week-old male BALB/c nude mice were purchased from the Experimental Animal Center at Sun Yat-sen University. A total of 3×10^6 SMMC-7721 cells were subcutaneously inoculated into the right flank of nude mice, to initiate tumor growth. When the tumor sizes reached ~3 × 3 mm, mice were randomly divided into four groups of six animals and treated intraperitoneally with LK-A (3 mg/kg and 6 mg/kg), 5-Fu (10mg/kg) or DMSO (negative control) dissolved in NaCl every 3 days for 4 weeks. Body weights and tumor volumes were measured every 3 days for 4 weeks. At the end of the study, animals were sacrificed and tumors were removed and weighed for use in immunohistochemistry experiments. The following formula was used to determine tumor volumes: tumor volume $= L \times W^2/2$, where L is the length and W the width. All animal handling and procedures were approved by the Ethical Committee of the Sun Yat-Sen University.

Tumor histology and immunohistochemistry. Isolated tumors and organ tissues were fixed in formalin and embedded in paraffin. Five micrometer sections were cut and stained with H&E. For immunohistochemical staining, sections were deparaffinized in xylene and hydrated through with graded alcohol, and endogenous peroxidase activity was blocked with 3% hydrogen peroxide for 10 min. Antigen retrieval was completed by cooking tissue sections for 3 min with citrate buffer (pH 6.0) for cleaved Caspase-3 and Skp2, and in EDTA buffer (pH 8.0) for Ki-67. Slides were incubated with 10% normal goat serum for 10 min at room temperature to block nonspecific binding, followed by incubation overnight with rabbit monoclonal antibody, anti-cleaved Caspase-3, Skp2 and mouse monoclonal antibody anti-Ki-67 at 4 °C in a moist chamber. Slides were washed twice with PBS and sequentially incubated with a secondary antibody for 30 min at room temperature, before staining with DAB (3, 3-diaminobenzidine). Finally, slides were counterstained with hematoxylin, dehydrated and mounted.

Statistical analysis. All data were expressed as mean ± standard deviation (S.D.) and statistically compared by one-way analysis of variance with Dunnett's test or unpaired Student's *t*-test in different experiments. A *P*-value of <0.05 was considered to be statistically significant.

Conflict of Interest

The authors declare no conflict of interest.

Acknowledgements. This study was supported by Grants from the National Natural Science Foundation of China (Nos 81225018, 81172340 and 81172939), and the West Light of Foundation of Chinese Academy of Sciences.

1. Rossi L, Zoratto F, Papa A, Iodice F, Minozzi M, Frati L *et al.* Current approach in the treatment of hepatocellular carcinoma. *World J Gastrointest Oncol* 2010; **2**: 348–359.
2. Tang TC, Man S, Lee CR, Xu P, Kerbel RS. Impact of metronomic UFT/cyclophosphamide chemotherapy and antiangiogenic drug assessed in a new preclinical model of locally advanced orthotopic hepatocellular carcinoma. *Neoplasia* 2010; **12**: 264–274.
3. Gamet-Payrastre L, Li P, Lumeau S, Cassar G, Dupont MA, Chevolleau S *et al.* Sulforaphane, a naturally occurring isothiocyanate, induces cell cycle arrest and apoptosis in HT29 human colon cancer cells. *Cancer Res* 2000; **60**: 1426–1433.
4. Snoek BC, de Wilt LH, Jansen G, Peters GJ. Role of E3 ubiquitin ligases in lung cancer. *World J Clin Oncol* 2013; **4**: 58–69.
5. Wei Z, Jiang X, Qiao H, Zhai B, Zhang L, Zhang Q *et al.* STAT3 interacts with Skp2/p27/p21 pathway to regulate the motility and invasion of gastric cancer cells. *Cell Signal* 2013; **25**: 931–938.
6. Uehara N, Yoshizawa K, Tsubura A. Vorinostat enhances protein stability of p27 and p21 through negative regulation of Skp2 and Cks1 in human breast cancer cells. *Oncol Rep* 2012; **28**: 105–110.
7. Su B, Chen X, Zhong C, Guo N, He J, Fan Y. All-trans retinoic acid inhibits mesangial cell proliferation by up-regulating p21Waf1/Cip1 and p27Kip1 and down-regulating Skp2. *J Nephrol* 2012; **25**: 1031–1040.
8. Carrano AC, Eytan E, Hershko A, Pagano M. SKP2 is required for ubiquitin-mediated degradation of the CDK inhibitor p27. *Nat Cell Biol* 1999; **1**: 193–199.
9. Nakayama K, Nagahama H, Minamishima YA, Matsumoto M, Nakamichi I, Kitagawa K *et al.* Targeted disruption of Skp2 results in accumulation of cyclin E and p27(Kip1), polyploidy and centrosome overduplication. *EMBO J* 2000; **19**: 2069–2081.
10. Ganoth D, Bornstein G, Ko TK, Larsen B, Tyers M, Pagano M *et al.* The cell-cycle regulatory protein Cks1 is required for SCF(Skp2)-mediated ubiquitinylation of p27. *Nat Cell Biol* 2001; **3**: 321–324.
11. Chen B, Zhao R, Su CH, Linan M, Tseng C, Phan L *et al.* CDK inhibitor p57 (Kip2) is negatively regulated by COP9 signalosome subunit 6. *Cell Cycle* 2012; **11**: 4633–4641.
12. Rodriguez S, Wang L, Mumaw C, Srour EF, Lo Celso C, Nakayama K *et al.* The SKP2 E3 ligase regulates basal homeostasis and stress-induced regeneration of HSCs. *Blood* 2011; **117**: 6509–6519.
13. Kitagawa K, Kotake Y, Kitagawa M. Ubiquitin-mediated control of oncogene and tumor suppressor gene products. *Cancer Sci* 2009; **100**: 1374–1381.
14. Pervaiz S, Clement MV. Tumor intracellular redox status and drug resistance–serendipity or a causal relationship? *Curr Pharm Des* 2004; **10**: 1969–1977.
15. Nicotera TM, Privalle C, Wang TC, Oshimura M, Barrett JC. Differential proliferative responses of Syrian hamster embryo fibroblasts to paraquat-generated superoxide radicals depending on tumor suppressor gene function. *Cancer Res* 1994; **54**: 3884–3888.
16. Murrell GA, Francis MJ, Bromley L. Modulation of fibroblast proliferation by oxygen free radicals. *Biochem J* 1990; **265**: 659–665.
17. Myatt SS, Brosens JJ, Lam EW. Sense and sensitivity: FOXO and ROS in cancer development and treatment. *Antioxid Redox Signal* 2011; **14**: 675–687.
18. Trachootham D, Alexandre J, Huang P. Targeting cancer cells by ROS-mediated mechanisms: a radical therapeutic approach? *Nat Rev Drug Discov* 2009; **8**: 579–591.
19. Wang H, Jiang D, Liu J, Ye S, Xiao S, Wang W *et al.* Compound K induces apoptosis of bladder cancer T24 cells *via* reactive oxygen species-mediated p38 MAPK pathway. *Cancer Biother Radiopharm* 2013; **28**: 607–614.
20. Zhao WX, Tang SS, Jin X, Zhang CM, Zhang T, Wang CC *et al.* Olaquindox-induced apoptosis is suppressed through p38 MAPK and ROS-mediated JNK pathways in HepG2 cells. *Cell Biol Toxicol* 2013; **29**: 229–238.
21. Sun HD, Huang SX, Han QB. Diterpenoids from Isodon species and their biological activities. *Nat Prod Rep* 2006; **23**: 673–698.
22. Wang WG, Li XN, Du X, Wu HY, Liu X, Su J *et al.* Laxiflorolides A and B, epimeric bishomoditerpene lactones from Isodon eriocalyx. *J Nat Prod* 2012; **75**: 1102–1107.
23. Wang WG, Du X, Li XN, Wu HY, Liu X, Shang SZ *et al.* New bicyclo[3.1.0]hexane unit ent-kaurane diterpene and its seco-derivative from Isodon eriocalyx var. laxiflora. *Org Lett* 2012; **14**: 302–305.
24. Wu ZY, Li XW. *Flora Repubulicae Popularis Sinicae*. vol 66. Science Press: Beijing, 1977.
25. Zou J, Du X, Pang G, Shi YM, Wang WG, Zhan R *et al.* Ternifolide A, a new diterpenoid possessing a rare macrolide motif from Isodon ternifolius. *Org Lett* 2012; **14**: 3210–3213.

26. Kullmann MK, Grubbauer C, Goetsch K, Jakel H, Podmirseg SR, Trockenbacher A *et al.* The p27-Skp2 axis mediates glucocorticoid-induced cell cycle arrest in T-lymphoma cells. *Cell Cycle* 2013; **12**: 2625–2635.
27. Sanchez N, Gallagher M, Lao N, Gallagher C, Clarke C, Doolan P *et al.* MiR-7 triggers cell cycle arrest at the G1/S transition by targeting multiple genes including Skp2 and Psme3. *PLoS One* 2013; **8**: e65671.
28. Huang Y, Tong S, Tai AW, Hussain M, Lok AS. Hepatitis B virus core promoter mutations contribute to hepatocarcinogenesis by deregulating SKP2 and its target, p21. *Gastroenterology* 2011; **141**: 1412–1421, 1421.e1–e5.
29. Fleury C, Mignotte B, Vayssiere JL. Mitochondrial reactive oxygen species in cell death signaling. *Biochimie* 2002; **84**: 131–141.
30. Remacle-Bonnet MM, Garrouste FL, Heller S, Andre F, Marvaldi JL, Pommier GJ. Insulin-like growth factor-I protects colon cancer cells from death factor-induced apoptosis by potentiating tumor necrosis factor alpha-induced mitogen-activated protein kinase and nuclear factor kappaB signaling pathways. *Cancer Res* 2000; **60**: 2007–2017.
31. Miyoshi N, Uchida K, Osawa T, Nakamura Y. A link between benzyl isothiocyanate-induced cell cycle arrest and apoptosis: involvement of mitogen-activated protein kinases in the Bcl-2 phosphorylation. *Cancer Res* 2004; **64**: 2134–2142.
32. Wang ZS, Luo P, Dai SH, Liu ZB, Zheng XR, Chen T *et al.* Induces apoptosis in human glioma U87 cells through p38-mediated ROS generation. *Cell Mol Neurobiol* 2013; **33**: 921–928.
33. Sawadogo WR, Schumacher M, Teiten MH, Dicato M, Diederich M. Traditional West African pharmacopeia, plants and derived compounds for cancer therapy. *Biochem Pharmacol* 2012; **84**: 1225–1240.
34. Xu HZ, Huang Y, Wu YL, Zhao Y, Xiao WL, Lin QS *et al.* Pharicin A, a novel natural ent-kaurene diterpenoid, induces mitotic arrest and mitotic catastrophe of cancer cells by interfering with BubR1 function. *Cell Cycle* 2010; **9**: 2897–2907.
35. Chiou CT, Kuo YH, Chan YY, Juang SH, Chan HH, Wu TS. Ajugalide-B (ATMA) is an anoikis-inducing agent from Ajuga taiwanensis with antiproliferative activity against tumor cells *in vitro*. *Phytochemistry* 2012; **80**: 64–69.
36. Gao FH, Hu XH, Li W, Liu H, Zhang YJ, Guo ZY *et al.* Oridonin induces apoptosis and senescence in colorectal cancer cells by increasing histone hyperacetylation and regulation of p16, p21, p27 and c-myc. *BMC Cancer* 2010; **10**: 610.
37. Li L, Yue GG, Lau CB, Sun H, Fung KP, Leung PC *et al.* Eriocalyxin B induces apoptosis and cell cycle arrest in pancreatic adenocarcinoma cells through caspase- and p53-dependent pathways. *Toxicol Appl Pharmacol* 2012; **262**: 80–90.
38. Zou QF, Du JK, Zhang H, Wang HB, Hu ZD, Chen SP *et al.* Anti-tumour activity of longikaurin A (LK-A), a novel natural diterpenoid, in nasopharyngeal carcinoma. *J Transl Med* 2013; **11**: 200.
39. Allan LA, Clarke PR. Phosphorylation of caspase-9 by CDK1/cyclin B1 protects mitotic cells against apoptosis. *Mol Cell* 2007; **26**: 301–310.
40. Booher RN, Holman PS, Fattaey A. Human Myt1 is a cell cycle-regulated kinase that inhibits Cdc2 but not Cdk2 activity. *J Biol Chem* 1997; **272**: 22300–22306.
41. Zhao Y, Wu Z, Zhang Y, Zhu L. HY-1 induces G2/M cell cycle arrest in human colon cancer cells through the ATR-Chk1-Cdc25C and Weel pathways. *Cancer Sci* 2013; **104**: 1062–1066.
42. Parker LL, Piwnica-Worms H. Inactivation of the p34cdc2-cyclin B complex by the human WEE1 tyrosine kinase. *Science* 1992; **257**: 1955–1957.
43. Abbas T, Dutta A. p21 in cancer: intricate networks and multiple activities. *Nat Rev Cancer* 2009; **9**: 400–414.
44. Taylor WR, Stark GR. Regulation of the G2/M transition by p53. *Oncogene* 2001; **20**: 1803–1815.
45. Boulaire J, Fotedar A, Fotedar R. The functions of the cdk-cyclin kinase inhibitor p21WAF1. *Pathol Biol (Paris)* 2000; **48**: 190–202.
46. Zhou W, Srinivasan S, Nawaz Z, Slingerland JM. ERα, SKP2 and E2F-1 form a feed forward loop driving late ERα targets and G1 cell cycle progression. *Oncogene* 2013; e-pub ahead of print 17 June 2013; doi:10.1038/onc.2013.197.
47. Qiao D, Meyer K, Friedl A. Glypican-1 stimulates Skp2 autoinduction loop and G1/S transition in endothelial cells. *J Biol Chem* 2012; **287**: 5898–5909.
48. Chan CH, Morrow JK, Li CF, Gao Y, Jin G, Moten A *et al.* Pharmacological inactivation of Skp2 SCF ubiquitin ligase restricts cancer stem cell traits and cancer progression. *Cell* 2013; **154**: 556–568.
49. Li S, Dong P, Wang J, Zhang J, Gu J, Wu X *et al.* Icariin, a natural flavonol glycoside, induces apoptosis in human hepatoma SMMC-7721 cells via a ROS/JNK-dependent mitochondrial pathway. *Cancer Lett* 2010; **298**: 222–230.
50. Ahmed K, Zaidi SF. Treating cancer with heat: hyperthermia as promising strategy to enhance apoptosis. *JPMA* 2013; **63**: 504–508.
51. Kuo PL, Chen CY, Hsu YL. Isoobtusilactone A induces cell cycle arrest and apoptosis through reactive oxygen species/apoptosis signal-regulating kinase 1 signaling pathway in human breast cancer cells. *Cancer Res* 2007; **67**: 7406–7420.
52. Trachootham D, Zhou Y, Zhang H, Demizu Y, Chen Z, Pelicano H *et al.* Selective killing of oncogenically transformed cells through a ROS-mediated mechanism by beta-phenylethyl isothiocyanate. *Cancer Cell* 2006; **10**: 241–252.
53. Raj L, Ide T, Gurkar AU, Foley M, Schenone M, Li X *et al.* Selective killing of cancer cells by a small molecule targeting the stress response to ROS. *Nature* 2011; **475**: 231–234.
54. Kong D, Zheng T, Zhang M, Wang D, Du S, Li X *et al.* Static mechanical stress induces apoptosis in rat endplate chondrocytes through MAPK and mitochondria-dependent caspase activation signaling pathways. *PLoS One* 2013; **8**: e69403.
55. Uchakina ON, Ban H, McKallip RJ. Targeting hyaluronic acid production for the treatment of leukemia: treatment with 4-methylumbelliferone leads to induction of MAPK-mediated apoptosis in K562 leukemia. *Leuk Res* 2013; **37**: 1294–1301.
56. Wang CL, Xia Y, Nie JZ, Zhou M, Zhang RP, Niu LL *et al.* Musca domestica larva lectin induces apoptosis in BEL-7402 cells through a Ca(2+)/JNK-mediated mitochondrial pathway. *Cell Biochem Biophys* 2013; **66**: 319–329.
57. Lee HJ, Auh QS, Lee YM, Kang SK, Chang SW, Lee DS *et al.* Growth inhibition and apoptosis-inducing effects of Cudraflavone B in human oral cancer cells via MAPK, NF-kappaB, and SIRT1 signaling pathway. *Planta Med* 2013; **79**: 1298–1306.
58. Shen HM, Liu ZG. JNK signaling pathway is a key modulator in cell death mediated by reactive oxygen and nitrogen species. *Free Radic Biol Med* 2006; **40**: 928–939.

Supplementary Information accompanies this paper on Cell Death and Disease website (http://www.nature.com/cddis)